



# Vibro-acoustic formulation of elastically restrained shear deformable stiffened rectangular plate

T.Y. Kam\*, C.H. Jiang, B.Y. Lee

Mechanical Engineering Department, National Chiao Tung University, Hsin Chu 300, Taiwan

## ARTICLE INFO

Article history:  
Available online 9 May 2012

Keywords:  
Acoustics  
Orthotropic plate  
Vibration  
Rayleigh–Ritz method  
Sound radiation

## ABSTRACT

A method constructed on the basis of the Rayleigh–Ritz method and the first Rayleigh integral is presented for the vibro-acoustic analysis of elastically restrained shear deformable stiffened rectangular orthotropic plates. In the proposed method, the displacement fields of the plate and stiffeners are formulated on the basis of the first-order shear deformation theory. The theoretical sound pressure level (SPL) curve of the plate is constructed using the responses at different excitation frequencies and the first Rayleigh integral. The experimental SPL curve of an elastically restrained stiffened orthotropic plate was measured to verify the accuracy of the theoretical SPL curve of the plate. The effects of Young's modulus ratio  $E_1/E_2$  on the sound radiation characteristics of elastically restrained stiffened orthotropic plate with different aspect ratios are studied using the proposed method. It has been shown that the effects of Young's modulus ratio become more prominent as the plate aspect ratio gets larger.

© 2012 Elsevier Ltd. All rights reserved.

## 1. Introduction

Because of their many advantages, composite plates have been used in different industries such as aero-space, aircraft, automobile, and audio industries to fabricate structures or sound radiators of high performance and reliability. In general, these plates are flexibly restrained at their edges or connected at their edges to members which can be treated as elastic restraints. Since the vibration of a plate is susceptible to sound radiation, the vibro-acoustic behaviors of plate structures have thus become an important topic of research. Recently, many papers [1–7] have been devoted to the vibro-acoustics of plates with regular boundary conditions subjected to various loads. In order to increase the stiffness of thin-walled structures without obvious increases in their weights, stiffeners are often used to reinforce the structures in some specifically chosen patterns. Because of their broad applications, the mechanical performance analysis of stiffened structures has become an important topic of research [8–16]. In particular, the vibro-acoustics of stiffened plates has been studied by a number of researchers [11–16]. Since, in practical applications, elastically restrained plates are important structural parts, a number of researchers have formulated some general methods for the vibro-acoustic analysis of elastically restrained rectangular thin isotropic plates [17–22]. As for the vibro-acoustics of elastically restrained stiffened composite plates, though important, not much attention has been drawn in this area.

In this paper, the vibro-acoustics, especially, the SPL curves of elastically restrained shear deformable stiffened orthotropic plates are studied via both theoretical and experimental approaches. The Rayleigh–Ritz method together with the first Rayleigh integral is used to study the vibro-acoustic behaviors and construct the SPL curves of elastically restrained shear deformable stiffened orthotropic plates. The accuracy of the proposed method will be verified by the experimental results obtained in this paper.

## 2. Plate vibration analysis

The stiffened rectangular orthotropic plate of size  $a$  (length)  $\times$   $b$  (width)  $\times$   $h_p$  (thickness) is elastically restrained along the plate periphery by distributed springs with translational and rotational spring constant intensities  $K_{Li}$  and  $K_{Ri}$ , respectively, and at the center by a spring of spring constant  $K_c$  as shown in Fig. 1. The  $x$ – $y$  plane of the reference coordinate is located at the mid-plane of the plate. It is noted that the plate is stiffened asymmetrically in  $x$  and  $y$  directions by a number of beams on the top and bottom surfaces of the plate. Herein, the displacements of the plate and stiffeners are modeled based on the first-order shear deformation theory. The displacement field of the plate is expressed as

$$\begin{aligned} u_p &= u_{op}(x, y, t) + Z_p \theta_{xp}(x, y, t) \\ v_p &= v_{op}(x, y, t) + Z_p \theta_{yp}(x, y, t) \\ w_p &= w_{op}(x, y, t) \end{aligned} \quad (1)$$

where  $u_p$ ,  $v_p$ , and  $w_p$  are the displacements in  $x$ ,  $y$ , and  $z$  directions, respectively;  $u_{op}$ ,  $v_{op}$ ,  $w_{op}$  are mid-plane displacements;  $\theta_{xp}$ ,  $\theta_{yp}$  are

\* Corresponding author.

E-mail address: [tykam@mail.nctu.edu.tw](mailto:tykam@mail.nctu.edu.tw) (T.Y. Kam).

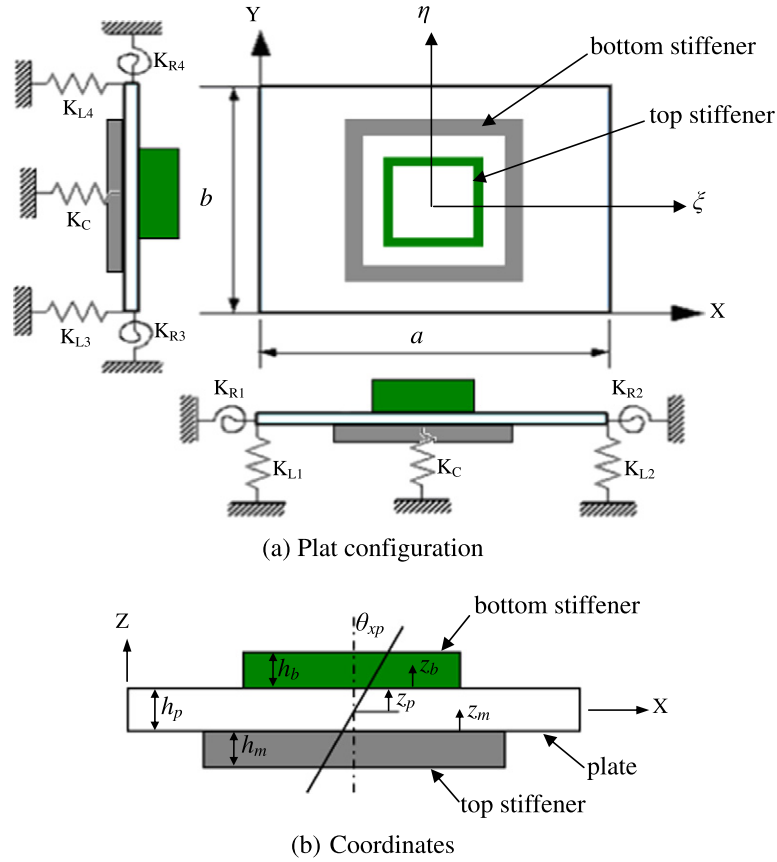


Fig. 1. Elastically restrained stiffened plate.

shear rotations. It is assumed that both the plate and stiffeners have same shear rotation. The strain–displacement relations of the plate are expressed as

$$\begin{aligned}
 \epsilon_x &= \frac{\partial u}{\partial x} = \frac{\partial u_{op}}{\partial x} + z_p \frac{\partial \theta_{xp}}{\partial x} \\
 \epsilon_y &= \frac{\partial v}{\partial y} = \frac{\partial v_{op}}{\partial y} + z_p \frac{\partial \theta_{yp}}{\partial y} \\
 \epsilon_z &= \frac{\partial w}{\partial z} = \frac{\partial w_{op}}{\partial z} = 0 \\
 \gamma_{yz} &= \frac{\partial v}{\partial z} + \frac{\partial w}{\partial y} = \theta_{yp} + \frac{\partial w_{op}}{\partial y} \\
 \gamma_{xz} &= \frac{\partial u}{\partial z} + \frac{\partial w}{\partial x} = \theta_{xp} + \frac{\partial w_{op}}{\partial x} \\
 \gamma_{xy} &= \frac{\partial u}{\partial y} + \frac{\partial v}{\partial x} = \left( \frac{\partial u_{op}}{\partial y} + \frac{\partial v_{op}}{\partial x} \right) + z_p \left( \frac{\partial \theta_{xp}}{\partial y} + \frac{\partial \theta_{yp}}{\partial x} \right)
 \end{aligned} \tag{2}$$

The stress–strain relations of the orthotropic plate are given as [23]

$$\begin{Bmatrix} \sigma_x \\ \sigma_y \\ \tau_{yz} \\ \tau_{xz} \\ \tau_{xy} \end{Bmatrix} = \begin{bmatrix} Q_{11} & Q_{12} & 0 & 0 & 0 \\ Q_{12} & Q_{22} & 0 & 0 & 0 \\ 0 & 0 & Q_{44} & 0 & 0 \\ 0 & 0 & 0 & Q_{55} & 0 \\ 0 & 0 & 0 & 0 & Q_{66} \end{bmatrix} \begin{Bmatrix} \epsilon_x \\ \epsilon_y \\ \gamma_{yz} \\ \gamma_{xz} \\ \gamma_{xy} \end{Bmatrix} \tag{3}$$

with

$$\begin{aligned}
 Q_{11} &= \frac{E_1}{1 - \nu_{12}\nu_{21}} \\
 Q_{12} &= \frac{\nu_{12}E_2}{1 - \nu_{12}\nu_{21}}
 \end{aligned}$$

$$\begin{aligned}
 Q_{22} &= \frac{E_2}{1 - \nu_{12}\nu_{21}} \\
 Q_{44} &= G_{23} \\
 Q_{55} &= G_{13} = G_{12} \\
 Q_{66} &= G_{12}
 \end{aligned} \tag{4}$$

where  $Q_{ij}$  is reduced stiffness constant,  $E_i$  is Young's modulus in the  $i$ th direction,  $\nu_{ij}$  is Poisson's ratio,  $G_{ij}$  is shear modulus.

The strain energy,  $U_p$ , of the plate is

$$U_p = \frac{1}{2} \int_{V_p} \left( \sigma_x \epsilon_x + \sigma_y \epsilon_y + \tau_{xy} \gamma_{xy} + \tau_{xz} \gamma_{xz} + \tau_{zy} \gamma_{yz} \right) dV_p \tag{5}$$

In view of the relations given in Eqs. (1)–(4), Eq. (5) can be rewritten as

$$\begin{aligned}
 U_p &= \frac{1}{2} \int_0^b \int_0^a \left\{ Q_{11} h_p \left( \frac{\partial u_{op}}{\partial x} \right)^2 + Q_{11} \frac{h_p^3}{12} \left( \frac{\partial \theta_{xp}}{\partial x} \right)^2 \right. \\
 &\quad + 2Q_{12} h_p \left( \frac{\partial u_{op}}{\partial x} \right) \left( \frac{\partial v_{op}}{\partial y} \right) + 2Q_{12} \frac{h_p^3}{12} \left( \frac{\partial \theta_{xp}}{\partial x} \right) \left( \frac{\partial \theta_{yp}}{\partial y} \right) \\
 &\quad + Q_{22} h_p \left( \frac{\partial v_{op}}{\partial y} \right)^2 + Q_{22} \frac{h_p^3}{12} \left( \frac{\partial \theta_{yp}}{\partial y} \right)^2 + Q_{66} K_p h_p \left( \frac{\partial u_{op}}{\partial y} \right)^2 \\
 &\quad + Q_{66} K_p h_p \left( \frac{\partial v_{op}}{\partial x} \right)^2 + Q_{66} K_p \frac{h_p^3}{12} \left( \frac{\partial \theta_{xp}}{\partial y} \right)^2 + Q_{66} K_p \frac{h_p^3}{12} \left( \frac{\partial \theta_{yp}}{\partial x} \right)^2 \\
 &\quad \left. + 2Q_{66} K_p h_p \left( \frac{\partial u_{op}}{\partial y} \right) \left( \frac{\partial v_{op}}{\partial x} \right) + 2Q_{66} K_p \frac{h_p^3}{12} \left( \frac{\partial \theta_{xp}}{\partial y} \right) \left( \frac{\partial \theta_{yp}}{\partial x} \right) \right\} dx dy
 \end{aligned}$$

$$\begin{aligned}
& + Q_{55}K_p h_p \theta_{xp}^2 + 2\theta_{xp} \frac{\partial w_{op}}{\partial x} + \left( \frac{\partial w_{op}}{\partial x} \right)^2 \\
& + Q_{44}K_p h_p \left[ \theta_{yp}^2 + 2\theta_{yp} \frac{\partial w_{op}}{\partial y} + \left( \frac{\partial w_{op}}{\partial y} \right)^2 \right] dx dy \quad (6)
\end{aligned}$$

where  $K_p$  is shear correction factor.

The kinetic energy,  $T_p$ , of the plate is

$$T_p = \frac{1}{2} \int_{V_p} \rho_p (\dot{u}_p^2 + \dot{v}_p^2 + \dot{w}_p^2) dV_p \quad (7)$$

where  $\rho_p$  is plate mass density. In view of Eq. (1), the above equation can be rewritten as

$$\begin{aligned}
T_p = \frac{1}{2} \int_0^a \int_0^b \rho_p \left[ h_p \left( \frac{\partial u_{op}}{\partial t} \right)^2 + \frac{1}{2} \frac{h_p^3}{12} \left( \frac{\partial \theta_{xp}}{\partial t} \right)^2 + h_p \left( \frac{\partial v_{op}}{\partial t} \right)^2 \right. \\
\left. + \frac{h_p^3}{12} \left( \frac{\partial \theta_{yp}}{\partial t} \right)^2 + h_p \left( \frac{\partial w_{op}}{\partial t} \right)^2 \right] dx dy \quad (8)
\end{aligned}$$

Regarding the stiffeners, the displacement field of a typical stiffener, for instance, a bottom stiffener oriented in  $x$ -direction is:

$$\begin{aligned}
u_{b3} &= u_{op}(x, t) + \frac{h_p}{2} \theta_{xp}(x, t) + z_b \theta_{xp}(x, t) \\
v_{b3} &= 0 \\
w_{b3} &= w_{op}(x, t)
\end{aligned} \quad (9)$$

where  $u_b$ ,  $v_b$ ,  $w_b$  are stiffener displacements. Here the lateral displacement of the stiffener is neglected and treated as zero. The strains and strain energy of the stiffener are given, respectively, as

$$\begin{aligned}
\varepsilon_x &= \frac{\partial u}{\partial x} = \frac{\partial u_{op}}{\partial x} + \frac{h_p}{2} \frac{\partial \theta_{xp}}{\partial x} + z_b \frac{\partial \theta_{xp}}{\partial x} \\
\varepsilon_y &= 0 \\
\varepsilon_z &= 0 \\
\gamma_{yz} &= 0 \\
\gamma_{xz} &= \frac{\partial u}{\partial z} + \frac{\partial w}{\partial x} = \theta_{xp} + \frac{\partial w_{op}}{\partial x} \\
\gamma_{xy} &= 0
\end{aligned} \quad (10)$$

and

$$\begin{aligned}
U_b = \int_{-\frac{L_b}{2}}^{\frac{L_b}{2}} \left[ \frac{1}{2} E_b h_b t_b \left( \frac{\partial u_{op}}{\partial x} \right)^2 + \frac{1}{8} E_b h_p^2 h_b t_b \left( \frac{\partial \theta_{xp}}{\partial x} \right)^2 + \frac{1}{6} E_b h_b^3 t_b \left( \frac{\partial \theta_{xp}}{\partial x} \right)^2 \right. \\
+ \frac{1}{2} E_b h_p t_b h_b \left( \frac{\partial u_{op}}{\partial x} \right) \left( \frac{\partial \theta_{xp}}{\partial x} \right) + \left( \frac{\partial \theta_{xp}}{\partial x} \right) - \frac{1}{2} t_b E_b h_b^2 \left( \frac{\partial u_{op}}{\partial x} \right) \left( \frac{\partial \theta_{xp}}{\partial x} \right) \\
+ \frac{1}{4} E_b h_p t_b h_b^2 \left( \frac{\partial \theta_{xp}}{\partial x} \right)^2 + \frac{1}{2} K_b G_b t_b h_b \theta_{xp}^2 + K_b G_b t_b h_b \theta_{xp} \left( \frac{\partial w_{op}}{\partial x} \right) \\
\left. + \frac{1}{2} K_b G_b t_b h_b \left( \frac{\partial w_{op}}{\partial x} \right)^2 \right] dx \quad (11)
\end{aligned}$$

where  $E_b$  is stiffener Young's modulus,  $L_b$  length,  $h_b$  height,  $t_b$  thickness,  $G_b$  shear modulus, and  $K_b$  shear correction factor. Here, it is assumed that  $K_p = K_b = 0.85$ . The kinetic energy of the stiffener is

$$T_b = \frac{1}{2} \int_{V_b} \rho_b \left[ \left( \frac{\partial u_{op}}{\partial t} - \frac{h_p}{2} \frac{\partial \theta_{xp}}{\partial t} + z_b \frac{\partial \theta_{xp}}{\partial t} \right)^2 + \left( \frac{\partial w_{op}}{\partial t} \right)^2 \right] dV_b \quad (12)$$

where  $\rho_b$  is stiffener mass density.

The strain energy,  $U_s$ , stored in the elastic restraints is written as

$$\begin{aligned}
U_s = \frac{K_{L1}}{2} \int_0^b w^2 \Big|_{x=0} dy + \frac{K_{L2}}{2} \int_0^b w^2 \Big|_{x=a} dy + \frac{K_{L3}}{2} \int_0^a w^2 \Big|_{y=0} dx \\
+ \frac{K_{L4}}{2} \int_0^a w^2 \Big|_{y=b} dx + \frac{K_{R1}}{2} \int_0^b (\theta_{xp})^2 \Big|_{x=0} dy \\
+ \frac{K_{R2}}{2} \int_0^b (\theta_{xp})^2 \Big|_{x=a} dy + \frac{K_{R3}}{2} \int_0^a (\theta_{yp})^2 \Big|_{y=0} dx \\
+ \frac{K_{R4}}{2} \int_0^a (\theta_{yp})^2 \Big|_{y=b} dx + K_c w \left( \frac{a}{2}, \frac{b}{2} \right)^2 \quad (13)
\end{aligned}$$

The total strain energy  $U$  and total kinetic energy  $T$  of the elastically restrained stiffened plate are written, respectively, as

$$U = U_p + \sum_{i=1}^{N_b} U_{bi} + \sum_{i=1}^{N_t} U_{ti} + U_s \quad (14)$$

and

$$T = T_p + \sum_{i=1}^{N_b} T_{bi} + \sum_{i=1}^{N_t} T_{ti} \quad (15)$$

where  $N_b$ ,  $N_t$  are numbers of bottom and top stiffeners, respectively.

The Rayleigh–Ritz method is used to study the free vibration of the elastically restrained stiffened plate. The displacements of the plate are expressed as

$$\begin{aligned}
u_0(x, y, t) &= U(x, y) \sin \omega t \\
v_0(x, y, t) &= V(x, y) \sin \omega t \\
w_0(x, y, t) &= W(x, y) \sin \omega t \\
\theta_x(x, y, t) &= \Theta_x(x, y) \sin \omega t \\
\theta_y(x, y, t) &= \Theta_y(x, y) \sin \omega t
\end{aligned} \quad (16)$$

with

$$\begin{aligned}
U(\xi, \eta) &= \sum_{i=1}^{\hat{A}} \sum_{j=1}^{\hat{B}} C_{ij} \phi_i(\xi) \varphi_j(\eta) \\
V(\xi, \eta) &= \sum_{i=1+\hat{A}j=1+\hat{B}}^{\hat{C}} \sum_{j=1+\hat{A}i=1+\hat{B}}^{\hat{D}} C_{ij} \phi_i(\xi) \varphi_j(\eta) \\
W(\xi, \eta) &= \sum_{i=1+\hat{C}j=1+\hat{D}}^{\hat{I}} \sum_{j=1+\hat{C}i=1+\hat{D}}^{\hat{J}} C_{ij} \phi_i(\xi) \varphi_j(\eta) \\
\Theta_x^{(1)}(\xi, \eta) &= \sum_{i=1+\hat{I}j=1+\hat{J}}^{\hat{M}} \sum_{j=1+\hat{I}i=1+\hat{J}}^{\hat{N}} C_{ij} \phi_i(\xi) \varphi_j(\eta) \\
\Theta_y^{(1)}(\xi, \eta) &= \sum_{i=1+\hat{M}j=1+\hat{N}}^{\hat{P}} \sum_{j=1+\hat{M}i=1+\hat{N}}^{\hat{Q}} C_{ij} \phi_i(\xi) \varphi_j(\eta)
\end{aligned} \quad (17)$$

where  $C_{ij}$  are unknown constants. Legendre's polynomials are used to represent the characteristic functions,  $\psi$  and  $\Psi$ . Let  $\xi = 2x/a - 1$  and  $\eta = 2y/b - 1$ . The normalized characteristic functions, for instance,  $\psi_i(\xi)$ , are given as

$$\begin{aligned} \phi_1(\xi) &= 1, \\ \phi_2(\xi) &= \xi, \quad -1 \leq \xi \leq 1 \end{aligned} \quad (18)$$

for  $n \geq 3$ ,

$$\phi_n(\xi) = [(2n - 3)\xi \times \phi_{n-1}(\xi) - (n - 2) \times \phi_{n-2}(\xi)] / (n - 1)$$

with the satisfaction of the following orthogonality condition:

$$\int_{-1}^1 \phi_n(\xi)\phi_m(\xi)d\xi = \begin{cases} 0, & \text{if } n \neq m \\ 2/2n - 1, & \text{if } n = m \end{cases} \quad (19)$$

Extremization of the functional  $\Pi = T - U$  gives the following eigenvalue problem.

$$[\mathbf{K} - \omega^2 \mathbf{M}] \mathbf{C} = 0 \quad (20)$$

where  $\mathbf{K}$  and  $\mathbf{M}$  are structural stiffness and mass matrices;  $\omega$  is circular frequency. The solution of the above eigenvalue problem can lead to the determination of the natural frequencies and mode shapes of the stiffened plate. The terms in  $\mathbf{K}$  and  $\mathbf{M}$  are listed in the appendix.

### 3. Plate sound radiation analysis

The modal characteristics obtained in the previous section can be used to study the force vibration and sound radiation of the elastically restrained stiffened plate. For a sound radiation panel excited by an electro-magnetic transducer with a cylindrical voice coil, the harmonic driving force  $F(t) = F_0 \sin \omega t$  is distributed uniformly around the periphery of the voice coil.

The equations of motion for the sound radiation plate subjected to forced vibration can be expressed as

$$\mathbf{M}\ddot{\mathbf{C}} + \mathbf{D}\dot{\mathbf{C}} + \mathbf{K}\mathbf{C} = \mathbf{F} \quad (21)$$

where  $\mathbf{F}$  is the force vector containing the following terms

$$\begin{aligned} F_{mn} &= \frac{F}{2\pi r_c} \int_0^{2\pi} \phi_m\left(\frac{2r_c}{a} \cos \theta\right) \varphi_n\left(\frac{2r_c}{b} \cos \theta\right) d\theta \sin \omega t, \\ &\text{for } m = 1 + \hat{C}, \dots, \hat{I}; \quad n = 1 + \hat{D}, \dots, \hat{J} \\ &= 0 \text{ for other } m, n \end{aligned} \quad (22)$$

The damping matrix  $\mathbf{D}$  is

$$[\mathbf{D}] = \alpha[\mathbf{M}] + \beta[\mathbf{K}] \quad (23)$$

with  $\alpha = \xi\omega$ ,  $\beta = 2\xi/\omega$  where  $\xi$  is damping ratio at the first resonant frequency of the elastically restrained plate. Eq. (23) can be solved using the modal analysis method.

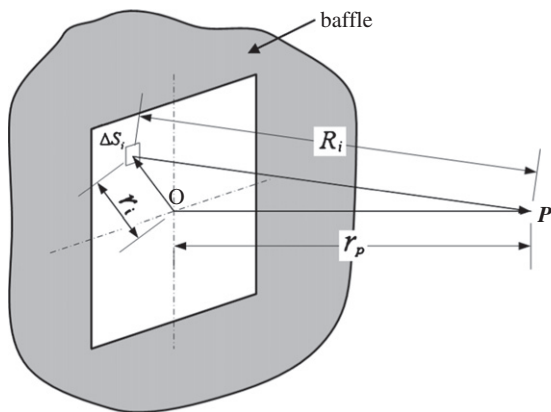


Fig. 2. Sound pressure measurement of baffled plate.

Referring to the baffled plate with area  $S$  shown in Fig. 2, if the effects of air loading on the plate vibration are neglected, the sound pressure  $p(r, t)$  resulting from the vibration of the plate can be determined using the first Rayleigh integral.

$$p(r, t) = \frac{-\omega^2 \rho_0}{2\pi} \sum_i A_i e^{j(2\pi t + \theta_i - kR_i)} \frac{\Delta S_i}{R_i} \quad (24)$$

where  $\rho_0$  is air density;  $k$  is wave number ( $=\omega/c$ ) with  $c$  being speed of sound;  $r_p$  is the distance between the plate center and the point of measurement;  $R_i = |r_p - r_i|$  the distance between the observation point and the position of the surface element at  $r_i$ ;  $\theta$  is phase angle;  $j = \sqrt{-1}$ . For air at 20 °C and standard atmospheric pressure,  $\rho_0 = 1.2 \text{ kg/m}^3$  and  $c = 344 \text{ m/s}$ . The SPL produced by the plate is calculated as

$$SPL \equiv 20 \log_{10} \left( \frac{p_{rms}}{2 \times 10^{-5}} \right) \text{ dB} \quad (25)$$

with

$$p_{rms} = \left[ \frac{1}{T} \int_{-T/2}^{T/2} |p(r, t)|^2 dt \right]^{1/2} \quad (26)$$

It is noted that both Eqs. (24) and (26) are solved numerically.

### 4. Experimental investigation

The sound radiation characteristics of the plate of size 26.6 mm × 20.8 mm × 1 mm, peripherally suspended by a flexible surround, and excited at the plate center by an electro-magnetic type exciter of 8 Ω impedance were investigated experimentally. On the top surface, the plate was stiffened by four beams in two different stiffening patterns, namely, Types I and II. For Type I

Table 1  
Properties of parts of elastically restrained stiffened plate.

Material constants	Plate	Surround	Stiffener
$E_1$ (GPa)	3.7		70
$E_2$ (GPa)	0.055		
$\nu_{12}$	0.03		0.33
$\nu_{23}$	0.2		
$\nu_{13}$	0.03		
$G_{12}$ (GPa)	0.05		
$G_{23}$ (GPa)	0.05/6		
$G_{13}$ (GPa)	0.05		
$\rho$ (kg/m <sup>3</sup> )	300		2790
$K_c$ (N/m <sup>2</sup> )		1654.4	
$K_l$ (N/m <sup>2</sup> )		4744.7	
$K_R$ (N)		0	

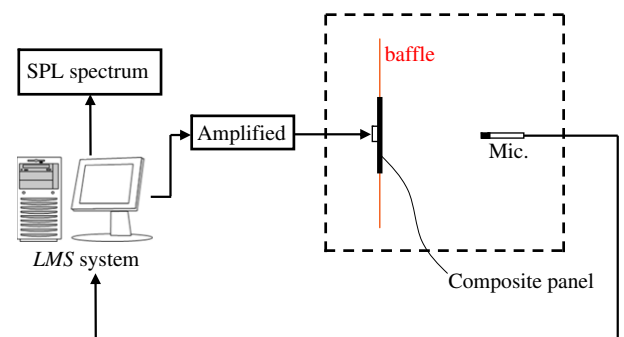


Fig. 3. Sound measurement apparatus.

stiffening pattern, the end points of the stiffeners of height ( $h_m$ ) 2.1 mm and thickness ( $t_m$ ) 2.5 mm were located at [6.25, 3.25], [-6.25, 3.25], [6.25, -3.25], and [-6.25, -3.25] mm, respectively. For Type II stiffening pattern, the end points of the stiffeners of height 1.33 mm and thickness 2.5 mm were located at [8.25, 6.75], [-8.25, 6.75], [8.25, -6.75], and [-8.25, -6.75] mm, respectively. The voice coil of the exciter was adhesively attached to the bottom surface of the plate. The properties of the voice coil of dimensions 9.35 (inner radius)  $\times$  6 (height  $h_b$ )  $\times$  0.05 (thickness  $t_b$ ) mm are given as

$$E = 0.129 \text{ GPa}, \quad \nu = 0.33, \quad \rho = 4403 \text{ Kg/m}^3 \quad (27)$$

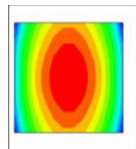
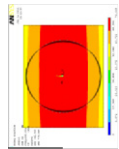
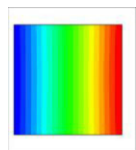
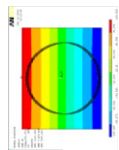
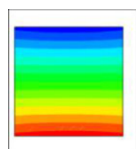
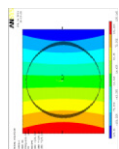
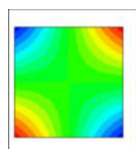
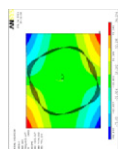
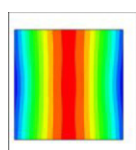
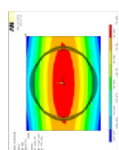
The properties of the plate, spring constant intensity of the surround (elastic restraint), and stiffeners are listed in Table 1. The experimental setup for measuring the sound radiation of the plate is shown schematically in Fig. 3 and the test was conducted in a semi-anechoic chamber. The sound pressure generated from the plate using one Watt power was measured by a microphone placed at the location one meter directly from the front surface of the plate. The sound pressure signals were then processed by LMS [24] to produce the SPL curve of the plate.

**5. Results and discussions**

The proposed method is first applied to study the free vibration of the elastically restrained orthotropic plate (aspect ratio  $a/b = 1.25$ ) which has been tested. In this study, the stiffeners on the top surface of the plate are removed from the plate. On the other hand, the voice coil is modeled by four stiffeners with their end points located, respectively, at [7.34, 7.34], [-7.34, 7.34], [7.34, -7.34], and [-7.34, -7.34] mm. It is noted that the perimeter of the voice coil is the same as the total length of the four beams. The convergence test has shown that the use of 10 terms of the characteristic functions for each displacement components can produce acceptable results. The first five natural frequencies and mode shapes of the plate stiffened by the voice coil are then determined using the present method. For comparison purpose, the finite element code ANSYS [25] is also used to determine the natural frequencies and mode shapes of the plate. In the finite element model, the element type Shell 99 is used to model the plate as well as the cylindrical voice coil. The results obtained using the present method and ANSYS are listed in Table 2 for comparison. It is noted that the present method and ANSYS have produced results in fairly good agreement and the maximum frequency difference between the two sets of results is less than 5%.

Next consider the effects of stiffening pattern on the sound radiation characteristics of the elastically restrained stiffened plate in the frequency range of 20 Hz–20 kHz. The theoretical SPL curves predicted using the present method are in comparison with the experimental ones for the plate with different stiffening patterns as shown in Figs. 4 and 5. It is noted that the theoretical and experimental SPL curves are in fairly good agreement. The discrepancies between the theoretical and experimental SPL curves, especially in the frequency range from 2 k to 20 kHz, are likely induced by the uncertainties involved in material damping, excitation force, imperfection of the semi-anechoic chamber, and material homogeneity of the orthotropic plate. The SPL curve of Type I stiffening pattern has two major SPL dips at around the frequencies of 1 kHz where the SPL drop is around 10 dB and 2 kHz where the SPL drop is around 7 dB. In general, such SPL dips are undesirable in the design of a high quality sound radiator. As for Type II stiffening pattern, except in the high frequency range, for instance, beyond 5 kHz, the SPL curve is relatively smooth comparing to that of Type I. The present method is then

**Table 2**  
Modal characteristics of elastically restrained orthotropic plate.

Method	Mode number	Natural frequency		Difference (%)
		Present	FEM	
Mode shape	1			4.15
	2			4.65
	3			3.90
	4			1.15
	5			4.46
Natural frequency	1	292.5	280.834	4.15
	2	412.2	393.874	4.65
	3	426.9	410.883	3.90
	4	873.4	863.497	1.15
	5	2595	2716	4.46

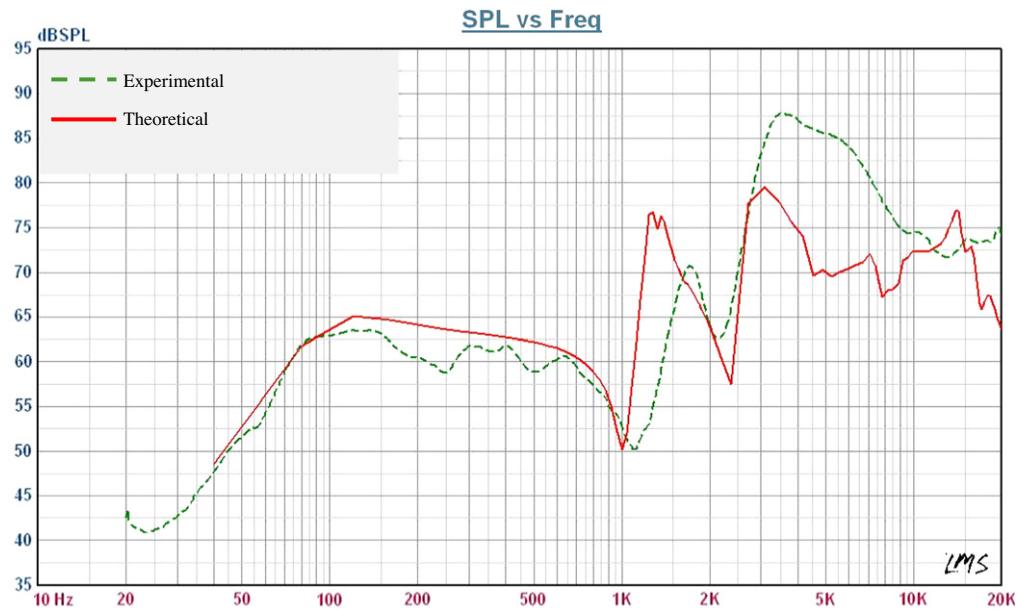


Fig. 4. Theoretical and experimental SPL curves of plate with Type I stiffening pattern.

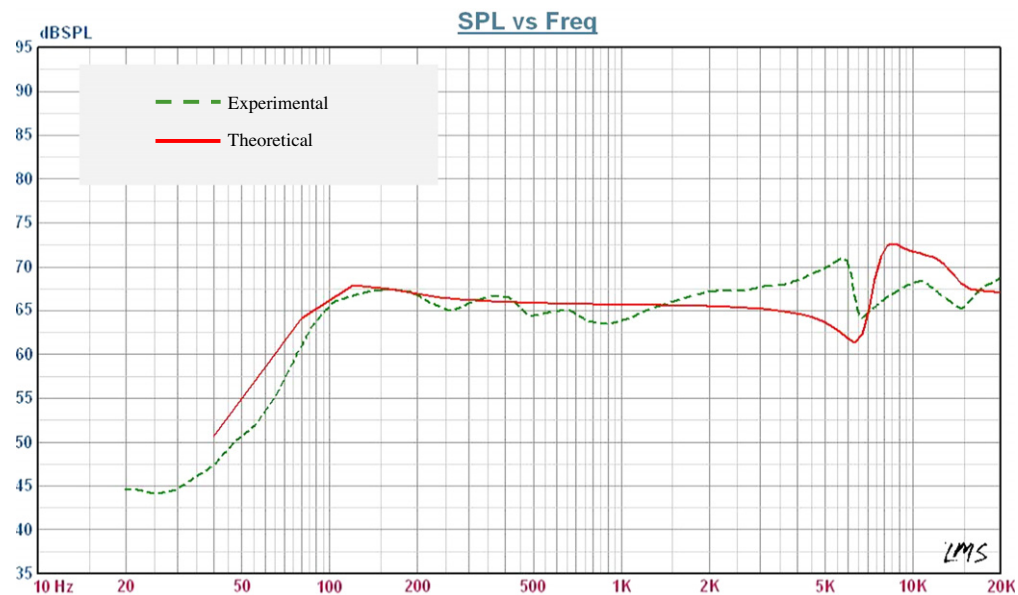


Fig. 5. Theoretical and experimental SPL curves of plate with Type II stiffening pattern.

used to study the effects of top stiffener's thickness on the SPL curve of the plate with Type II stiffening pattern. The SPL curves of the plate for different top stiffener heights are shown in Fig. 6. It is noted that as expected, when the stiffener height increases, the sensitivity of the SPL curve will decrease. The decrease of SPL curve is mainly due to the increase in the plate weight. The increase in the stiffener's moment of inertia, however, has negligible effects on the shape of the SPL curve.

Finally, the effects of the ratio of the plate Young's moduli ( $E_1/E_2$ ) on the SPL curve of the stiffened plate are studied by means of a number of numerical examples. Now the end points of the top stiffeners for the plate of  $a/b = 1.25$  are located at

$[9.25, 7.75]$ ,  $[-9.25, 7.75]$ ,  $[9.25, -7.75]$ , and  $[-9.25, -7.75]$ , respectively. The height and thickness of the stiffeners are 1.17 mm and 2.5 mm, respectively. Setting  $E_2 = 0.055$  GPa, the SPL curves for  $E_1/E_2 = 1, 2,$  and  $3$  are shown in Fig. 7 for comparison. On the other hand, setting  $E_1 = 3.7$  GPa, the SPL curves for  $E_1/E_2 = 1, 1/2,$  and  $1/3$  are shown in Fig. 8 for comparison. It is noted that for both cases, the small variations of the SPL curves in the high frequency range for these cases have demonstrated the fact that  $E_1/E_2$  has negligible effects on the sound radiation characteristics of the plate with  $a/b = 1.25$  when the top stiffeners are at the optimal locations. To study the effects of  $a/b$  on the sound radiation characteristics of orthotropic plates, the present

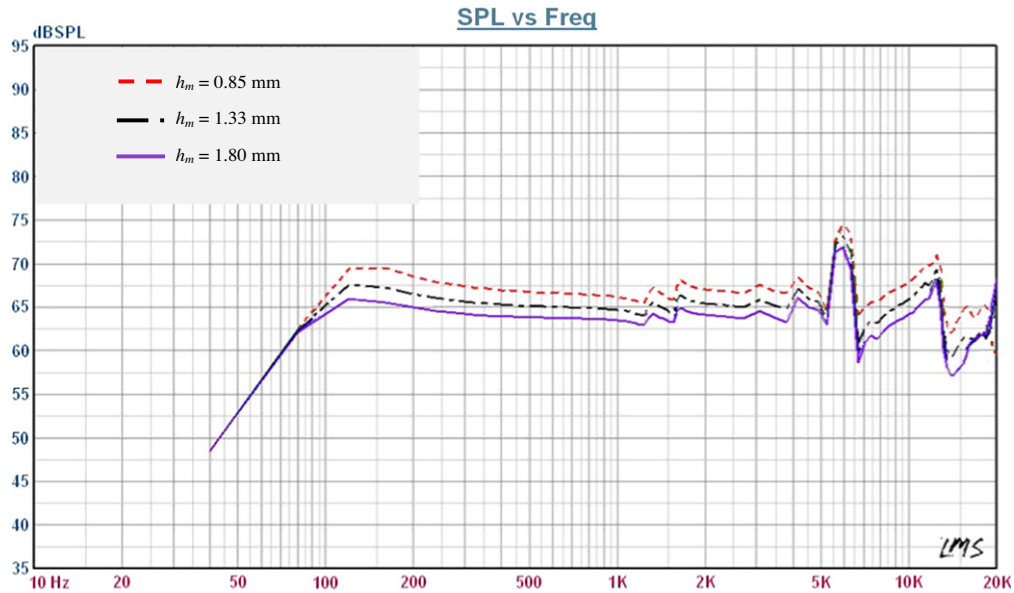


Fig. 6. SPL curves for Type II stiffening pattern with different top stiffener thicknesses ( $a/b = 1.25$ ).

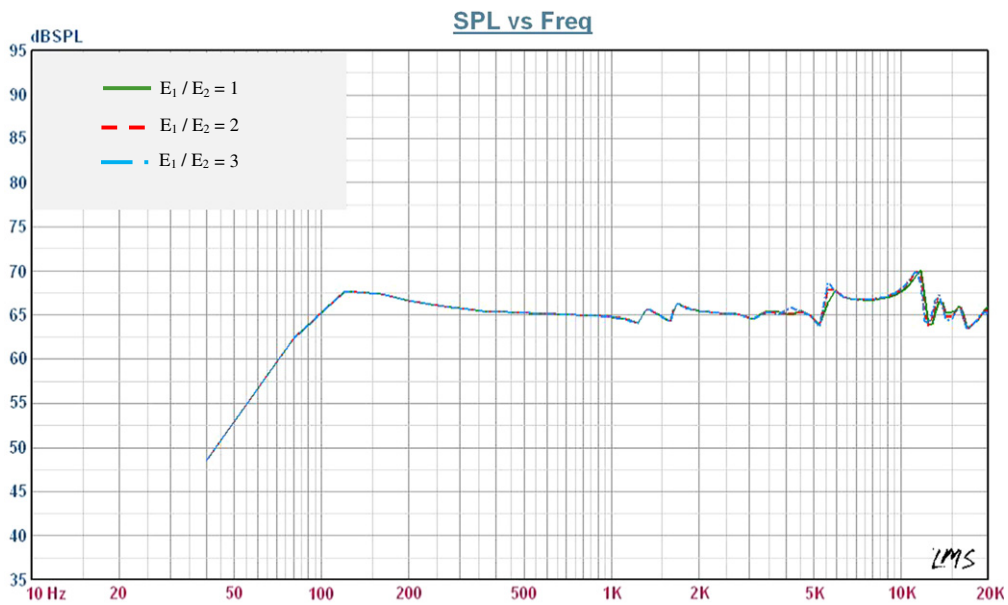


Fig. 7. SPL curves of stiffened plate with different  $E_1/E_2$  ( $a/b = 1.25$ ,  $E_2 = 0.055$  GPa).

method is used to predict the SPL curve of an elastically restrained stiffened orthotropic plates of  $a/b = 2.92$  with  $a = 76$  mm,  $b = 26$  mm and  $h_p = 1.3$  mm. The voice coil of radius 12.7 mm is modeled as four stiffeners with end points located at  $[20.03, 20.03]$ ,  $[-20.03, 20.03]$ ,  $[20.03, -20.03]$ , and  $[-20.03, -20.03]$  mm. Setting  $E_2 = 0.055$  GPa, the SPL curves for  $E_1/E_2 = 1$ ,  $1/2$ , and  $1/3$  are shown in Fig. 9 for comparison. It is noted that the first major SPL dip at 850 Hz for  $E_1/E_2 = 1$  moves to lower frequency range as  $E_1/E_2$  becomes less than 1. The frequency shift of the first major SPL dip is mainly due to the stiffness decrease in the  $x$ -direction. Since the mode shape for the first major SPL dip

remains the same, the mere decrease or increase in  $E_1/E_2$  cannot completely remove the SPL dip.

## 6. Conclusion

A method based on the Rayleigh–Ritz method and the Rayleigh first integral has been developed for the vibro-acoustic analysis of elastically restrained stiffened rectangular plates. The accuracy of the proposed method in predicting the SPL curve of an elastically restrained stiffened orthotropic plate of aspect ratio  $a/b = 1.25$  has been verified by the measured SPL curve. The effects of Young's

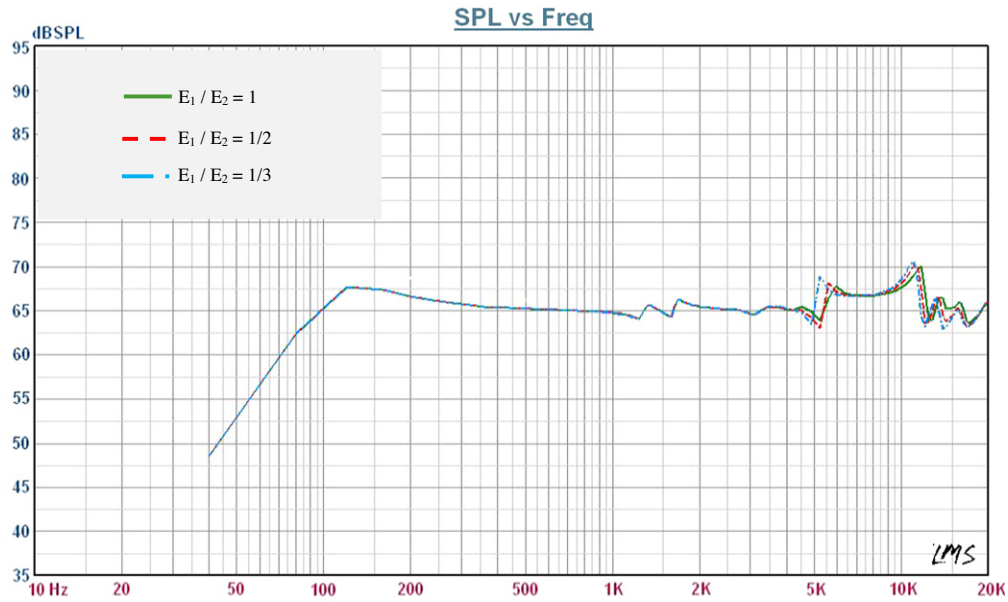


Fig. 8. SPL curves of stiffened plate with different  $E_1/E_2$  ( $a/b = 1.25$ ,  $E_1 = 3.7$  GPa).

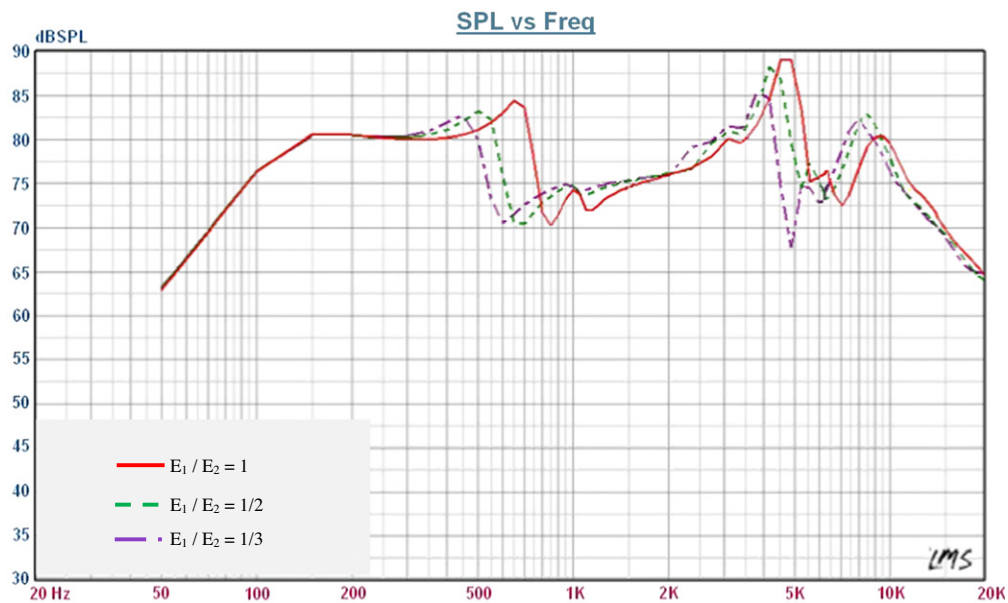


Fig. 9. SPL curves of stiffened plate with different  $E_1/E_2$  ( $a/b = 2.92$ ,  $E_2 = 0.055$  GPa).

modulus ratio  $E_1/E_2$  and aspect ratio  $a/b$  on the SPL curves of elastically restrained stiffened rectangular orthotropic plates have been studied using the proposed method. It has been shown that the effects of Young's modulus ratio on the SPL curve of the plate of aspect ratio  $a/b = 1.25$  is negligible. On the contrary, the decrease in Young's modulus ratio can move the frequency of the mid-frequency range dip to lower frequency range for the plate of aspect ratio  $a/b = 2.92$ .

**Acknowledgement**

The work of this paper has been supported by the National Science Council of the Republic of China under Grant NSC 100-2221-E-009-135.

**Appendix A**

$$\begin{pmatrix} K^{11} & K^{12} & K^{13} & 0 & 0 \\ K^{21} & K^{22} & K^{23} & K^{24} & K^{25} \\ K^{31} & K^{32} & K^{33} & K^{34} & K^{35} \\ 0 & K^{42} & K^{43} & K^{44} & K^{45} \\ 0 & K^{52} & K^{53} & K^{54} & K^{55} \end{pmatrix} - \omega^2 \begin{pmatrix} M^{11} & 0 & 0 & 0 & 0 \\ 0 & M^{22} & 0 & 0 & M^{25} \\ 0 & 0 & M^{33} & M^{34} & 0 \\ 0 & 0 & M^{43} & M^{44} & 0 \\ 0 & M^{52} & 0 & 0 & M^{55} \end{pmatrix} \begin{pmatrix} C_{ij} \\ C_{pq} \\ C_{mn} \\ C_{ab} \\ C_{cd} \end{pmatrix} = \begin{pmatrix} 0 \\ 0 \\ 0 \\ 0 \\ 0 \\ 0 \\ 0 \end{pmatrix} \tag{A1}$$



with  $N_b = N_t = 4$  and

$$\begin{aligned}
 [K^{11}]_{ijij} = & \left( \frac{4}{a^2} K_p h_p Q_{55} E_{ii}^{11} F_{jj}^{00} + \frac{4}{b^2} K_p h_p Q_{44} E_{ii}^{00} F_{jj}^{11} \right) \frac{ab}{4} \\
 & + \frac{1}{2} \left( K_{L_1} b F_{ij}^{00} B B_{ii}^{00} + K_{L_2} b F_{ij}^{00} B B_{ii}^{00} + K_{L_3} a E_{ii}^{00} B B_{ij}^{00} + K_{L_4} a E_{ii}^{00} B B_{ij}^{00} \right) \\
 & + K_C E_{ii}^{00} F_{jj}^{00} + \frac{2}{a} K_b G_b A_b \left( B e f_{ij}^{11} B e_{ii}^{00} + B e f_{ij}^{11} B f_{ii}^{00} \right) \\
 & + \frac{2}{b} K_b G_b A_b \left( B c_{ij}^{00} B c d_{ii}^{11} + B d_{ij}^{00} B c d_{ii}^{11} \right) \\
 & + \frac{2}{a} K_m G_m A_m \left( M e f_{ij}^{11} M e_{ii}^{00} + M e f_{ij}^{11} M f_{ii}^{00} \right) \\
 & + \frac{2}{b} K_m G_m A_m \left( M c_{ij}^{00} M c d_{ii}^{11} + M d_{ij}^{00} M c d_{ii}^{11} \right) \quad (A2)
 \end{aligned}$$

$$\begin{aligned}
 [K^{12}]_{ijmn} = & \left( \frac{2}{b} K_p h_p Q_{44} E_{im}^{00} F_{jn}^{10} \right) \frac{ab}{4} + K_b G_b A_b \left( B c_{jm}^{00} B c d_{im}^{10} + B d_{jm}^{00} B c d_{im}^{10} \right) \\
 & + K_m G_m A_m \left( M c_{jm}^{00} M c d_{im}^{10} + M d_{jm}^{00} M c d_{im}^{10} \right)
 \end{aligned}$$

$$\begin{aligned}
 [K^{13}]_{ijpq} = & \left( \frac{2}{a} K_p h_p Q_{55} E_{ip}^{10} F_{jq}^{00} \right) \frac{ab}{4} + K_b G_b A_b \left( B e f_{jq}^{10} B e_{ip}^{00} + B e f_{jq}^{10} B f_{ip}^{00} \right) \\
 & + K_m G_m A_m \left( M e f_{jq}^{10} M e_{ip}^{00} + M e f_{jq}^{10} M f_{ip}^{00} \right)
 \end{aligned}$$

$$\begin{aligned}
 [K^{22}]_{mnmn} = & \left( \frac{4}{b^2} \frac{h_p^3}{12} Q_{22} E_{mn}^{00} F_{nn}^{11} + \frac{h_p^3}{3a^2} Q_{66} E_{mn}^{11} F_{nn}^{00} + K_p h_p Q_{44} E_{mn}^{00} F_{nn}^{00} \right) \frac{ab}{4} \\
 & + \left( \frac{h_p^2}{2b} E_b A_b + \frac{2h_b^2}{3b} E_b A_b + E_b h_p A_b \frac{h_b}{b} \right) \left( B c_{nn}^{00} B c d_{mm}^{11} + B d_{nn}^{00} B c d_{mm}^{11} \right) \\
 & + \frac{b}{2} K_b G_b A_b \left( B c_{nn}^{00} B c d_{mm}^{00} + B d_{nn}^{00} B c d_{mm}^{00} \right) \\
 & + \left( \frac{h_p^2}{2b} E_m A_m + \frac{2h_m^2}{3b} E_m A_m + E_m h_m A_m \frac{h_m}{b} \right) \\
 & \times \left( M c_{nn}^{00} M c d_{mm}^{11} + M d_{nn}^{00} M c d_{mm}^{11} \right) \\
 & + \frac{b}{2} K_m G_m A_m \left( M c_{nn}^{00} M c d_{mm}^{00} + M d_{nn}^{00} M c d_{mm}^{00} \right)
 \end{aligned}$$

$$[K^{23}]_{mnpq} = \left( \frac{4}{ab} \frac{h_p^3}{12} Q_{12} E_{mp}^{01} F_{nq}^{10} + \frac{h_p^3}{3ab} Q_{66} E_{mp}^{10} F_{nq}^{01} \right) \frac{ab}{4}$$

$$\begin{aligned}
 [K^{25}]_{mncd} = & \left( \frac{h_p}{b} A_b E_b + \frac{h_b}{b} A_b E_b \right) \left( B c_{nd}^{00} B c d_{mc}^{11} + B d_{nd}^{00} B c d_{mc}^{11} \right) \\
 & - \left( \left( \frac{h_p}{b} A_m E_m + \frac{h_m}{b} A_m E_m \right) \left( M c_{nd}^{00} M c d_{mc}^{11} + M d_{nd}^{00} M c d_{mc}^{11} \right) \right)
 \end{aligned}$$

$$\begin{aligned}
 [K^{33}]_{pq\bar{p}\bar{q}} = & \left( \frac{4}{a^2} \frac{h_p^3}{12} Q_{11} E_{pp}^{11} F_{qq}^{00} + \frac{h_p^3}{3b^2} Q_{66} E_{pp}^{00} F_{qq}^{11} + K_p h_p Q_{55} E_{pp}^{00} F_{qq}^{00} \right) \frac{ab}{4} \\
 & + \left( \frac{h_p^2}{2a} E_b A_b + \frac{2h_b^2}{3a} E_b A_b + E_b h_p A_b \frac{h_b}{a} \right) \\
 & \times \left( B e f_{qq}^{11} B e_{pp}^{00} + B e f_{qq}^{11} B f_{pp}^{00} \right) \\
 & + \frac{a}{2} K_b G_b A_b \left( B e f_{qq}^{00} B e_{pp}^{00} + B e f_{qq}^{00} B f_{pp}^{00} \right) \\
 & + \left( \frac{h_p^2}{2a} E_m A_m + \frac{2h_m^2}{3a} E_m A_m + E_m h_m A_m \frac{h_p}{a} \right) \\
 & \times \left( M e f_{qq}^{11} M e_{pp}^{00} + M e f_{qq}^{11} M f_{pp}^{00} \right) \\
 & + \frac{a}{2} K_m G_m A_m \left( M e f_{qq}^{00} M e_{pp}^{00} + M e f_{qq}^{00} M f_{pp}^{00} \right)
 \end{aligned}$$

$$\begin{aligned}
 [K^{34}]_{pqab} = & \left( \frac{h_p}{a} A_b E_b + \frac{h_b}{a} A_b E_b \right) \left( B e f_{qb}^{11} B e_{pa}^{00} + B e f_{qb}^{11} B f_{pa}^{00} \right) \\
 & - \left( \left( \frac{h_p}{a} A_m E_m + \frac{h_m}{a} A_m E_m \right) \left( M e f_{qb}^{11} M e_{pa}^{00} + M e f_{qb}^{11} M f_{pa}^{00} \right) \right)
 \end{aligned}$$

$$\begin{aligned}
 [K^{44}]_{ab\bar{a}\bar{b}} = & \left( \frac{4h_p}{a^2} Q_{11} E_{aa}^{11} F_{bb}^{00} + \frac{4h_p}{b^2} Q_{66} E_{aa}^{00} F_{bb}^{11} \right) \frac{ab}{4} \\
 & + \left( \frac{2}{a} E_b A_b \right) \left( B e f_{bb}^{11} B e_{aa}^{00} + B e f_{bb}^{11} B f_{aa}^{00} \right) \\
 & + \left( \frac{2}{a} E_m A_m \right) \left( M e f_{bb}^{11} M e_{aa}^{00} + M e f_{bb}^{11} M f_{aa}^{00} \right)
 \end{aligned}$$

$$[K^{45}]_{abcd} = \left( \frac{4}{ab} \frac{h_p}{12} Q_{12} E_{ac}^{01} F_{bd}^{10} + \frac{4h_p}{ab} Q_{66} E_{ac}^{10} F_{bd}^{01} \right) \frac{ab}{4}$$

$$\begin{aligned}
 [K^{55}]_{cd\bar{c}\bar{d}} = & \left( \frac{4h_p}{b^2} Q_{22} E_{cc}^{00} F_{db}^{11} + \frac{4h_p}{a^2} Q_{66} E_{cc}^{11} F_{db}^{00} \right) \frac{ab}{4} \\
 & + \left( \frac{2}{b} E_b A_b \right) \left( B c_{db}^{00} B c d_{cc}^{11} + B d_{db}^{00} B c d_{cc}^{11} \right) \\
 & + \left( \frac{2}{b} E_m A_m \right) \left( M c_{db}^{00} M c d_{cc}^{11} + M d_{db}^{00} M c d_{cc}^{11} \right)
 \end{aligned}$$

and

$$\begin{aligned}
 [M^{11}]_{ijij} = & \left( \rho_p h_p E_{ii}^{00} F_{jj}^{00} \right) \frac{ab}{4} + \frac{a}{2} \rho_b A_b \left( B e f_{ij}^{00} B e_{ii}^{00} + B e f_{ij}^{00} B f_{ii}^{00} \right) \\
 & + \frac{b}{2} \rho_b A_b \left( B c_{ij}^{00} B c d_{ii}^{00} + B d_{ij}^{00} B c d_{ii}^{00} \right) \\
 & + \frac{a}{2} \rho_m A_m \left( M e f_{ij}^{00} M e_{ii}^{00} + M e f_{ij}^{00} M f_{ii}^{00} \right) \\
 & + \frac{b}{2} \rho_m A_m \left( M c_{ij}^{00} M c d_{ii}^{00} + M d_{ij}^{00} M c d_{ii}^{00} \right)
 \end{aligned}$$

$$\begin{aligned}
 [M^{22}]_{mnmn} = & \left( \rho_p \frac{h_p^3}{12} E_{mn}^{00} F_{nn}^{00} \right) \frac{ab}{4} \\
 & + \left( \frac{h_p^2 b}{8} \rho_b A_b + \frac{h_b^2 b}{6} \rho_b A_b + \frac{h_b b}{4} \rho_b A_b \right) \\
 & \times \left( B c_{nn}^{00} B c d_{mm}^{00} + B d_{nn}^{00} B c d_{mm}^{00} \right) \\
 & + \left( \frac{h_p^2 b}{8} \rho_m A_m + \frac{h_m^2 b}{6} \rho_m A_m + \frac{h_m b}{4} \rho_m A_m \right) \\
 & \times \left( M c_{nn}^{00} M c d_{mm}^{00} + M d_{nn}^{00} M c d_{mm}^{00} \right)
 \end{aligned}$$

$$\begin{aligned}
 [M^{25}]_{mncd} = & \left( b \rho_b A_b \frac{h_p}{4} + b \rho_b A_b \frac{h_b}{4} \right) \left( B c_{nd}^{00} B c d_{mc}^{00} + B d_{nd}^{00} B c d_{mc}^{00} \right) \\
 & - \left( b \rho_m A_m \frac{h_p}{4} + b \rho_m A_m \frac{h_m}{4} \right) \left( M c_{nd}^{00} M c d_{mc}^{00} + M d_{nd}^{00} M c d_{mc}^{00} \right)
 \end{aligned}$$

$$\begin{aligned}
 [M^{33}]_{pq\bar{p}\bar{q}} = & \left( \rho_p \frac{h_p^3}{12} E_{pp}^{00} F_{qq}^{00} \right) \frac{ab}{4} \\
 & + \left( \frac{h_p^2 a}{8} \rho_b A_b + \frac{h_b^2 a}{6} \rho_b A_b + \frac{h_b a}{4} \rho_b A_b \right) \\
 & \times \left( B e f_{qq}^{00} B e_{pp}^{00} + B e f_{qq}^{00} B f_{pp}^{00} \right) \\
 & + \left( \frac{h_p^2 a}{8} \rho_m A_m + \frac{h_m^2 a}{6} \rho_m A_m + \frac{h_m a}{4} \rho_m A_m \right) \\
 & \times \left( M e f_{qq}^{00} M e_{pp}^{00} + M e f_{qq}^{00} M f_{pp}^{00} \right) \quad (A3)
 \end{aligned}$$

$$[M^{34}]_{pqab} = \left( a\rho_b A_b \frac{h_p}{4} + a\rho_b A_b \frac{h_b}{4} \right) \left( Bef_{qb}^{00} Be_{pa}^{00} + Bef_{qb}^{00} Bf_{pa}^{00} \right) - \left( a\rho_m A_m \frac{h_p}{4} + a\rho_m A_m \frac{h_m}{4} \right) \left( Mef_{qb}^{00} Me_{pa}^{00} + Mef_{qb}^{00} Mf_{pa}^{00} \right)$$

$$Me_{im}^{rs} = \varphi_i^r \left( \eta = \frac{-L_1}{b} \right) \varphi_m^s \left( \eta = \frac{-L_1}{b} \right) \\ Mf_{im}^{rs} = \varphi_i^r \left( \eta = \frac{L_1}{b} \right) \varphi_m^s \left( \eta = \frac{L_1}{b} \right) \quad (A5)$$

$$[M^{44}]_{ab\bar{a}\bar{b}} = \left( \rho_p h_p E_{aa}^{00} F_{bb}^{00} \right) + \left( \frac{a}{2} \rho_b A_b \right) \left( Bef_{bb}^{00} Be_{aa}^{00} + Bef_{bb}^{00} Bf_{aa}^{00} \right) + \left( \frac{a}{2} \rho_m A_m \right) \left( Mef_{bb}^{00} Me_{aa}^{00} + Mef_{bb}^{00} Mf_{aa}^{00} \right)$$

$$[M^{55}]_{cd\bar{c}\bar{d}} = \left( \rho_p h_p E_{cc}^{00} F_{db}^{00} \right) + \left( \frac{b}{2} \rho_b A_b \right) \left( Bc_{db}^{00} Bcd_{cc}^{00} + Bd_{db}^{00} Bcd_{cc}^{00} \right) + \left( \frac{b}{2} \rho_m A_m \right) \left( Mc_{db}^{00} Mcd_{cc}^{00} + Md_{db}^{00} Mcd_{cc}^{00} \right)$$

there

$$r, s = 0, 1; i, j, \bar{i}, \bar{j} = 1, 2, 3, \dots, I, J \\ m, n, \bar{m}, \bar{n} = 1, 2, 3, \dots, M, N \\ p, q, \bar{p}, \bar{q} = 1, 2, 3, \dots, P, Q \\ a, b, \bar{a}, \bar{b} = 1, 2, 3, \dots, A, B \\ c, d, \bar{c}, \bar{d} = 1, 2, 3, \dots, C, D \quad (A4)$$

$$E_{im}^{rs} = \int_{-1}^1 \left[ \frac{d^r \phi_i(\xi)}{d\xi^r} \frac{d^s \phi_m(\xi)}{d\xi^s} \right] d\xi; \dots; F_{jn}^{rs} = \int_{-1}^1 \left[ \frac{d^r \varphi_j(\eta)}{d\eta^r} \frac{d^s \varphi_n(\eta)}{d\eta^s} \right] d\eta$$

$$Bcd_{im}^{rs} = \int_{-\frac{L_2}{a}}^{\frac{L_2}{a}} \phi_i^r(\xi) \phi_m^s(\xi) d\xi$$

$$Mcd_{im}^{rs} = \int_{-\frac{L_2}{a}}^{\frac{L_2}{a}} \phi_i^r(\xi) \phi_m^s(\xi) d\xi$$

$$Bef_{im}^{rs} = \int_{\frac{-L_1}{b}}^{\frac{L_1}{b}} \varphi_i^r(\eta) \varphi_m^s(\eta) d\eta$$

$$Mef_{im}^{rs} = \int_{\frac{-L_1}{b}}^{\frac{L_1}{b}} \varphi_i^r(\eta) \varphi_m^s(\eta) d\eta$$

$$Bc_{im}^{rs} = \phi_i^r \left( \xi = \frac{-L_2}{a} \right) \phi_m^s \left( \xi = \frac{-L_2}{a} \right)$$

$$Bd_{im}^{rs} = \phi_i^r \left( \xi = \frac{L_2}{a} \right) \phi_m^s \left( \xi = \frac{L_2}{a} \right)$$

$$Be_{im}^{rs} = \varphi_i^r \left( \eta = \frac{-L_1}{b} \right) \varphi_m^s \left( \eta = \frac{-L_1}{b} \right)$$

$$Bf_{im}^{rs} = \varphi_i^r \left( \eta = \frac{L_1}{b} \right) \varphi_m^s \left( \eta = \frac{L_1}{b} \right)$$

$$Mc_{im}^{rs} = \phi_i^r \left( \xi = \frac{-L_2}{a} \right) \phi_m^s \left( \xi = \frac{-L_2}{a} \right)$$

$$Md_{im}^{rs} = \phi_i^r \left( \xi = \frac{L_2}{a} \right) \phi_m^s \left( \xi = \frac{L_2}{a} \right)$$

### References

- [1] Li S. Active modal control simulation of vibro-acoustic response of a fluid-loaded plate. *J Sound Vib* 2011;330(23):5545–57.
- [2] Putra A, Thompson DJ. Radiation efficiency of unbaffled and perforated plates near a rigid reflecting surface. *J Sound Vib* 2011;330(22):5443–59.
- [3] Jeyaraj P, Padmanabhan C, Ganesan N. Vibro-acoustic behavior of a multilayered viscoelastic sandwich plate under a thermal environment. *J Sandwich Struct Mater* 2011;13(5):509–37.
- [4] Inalpolat M, Caliskan M, Sing R. Analysis of near field sound radiation from a resonant unbaffled plate using simplified analytical models. *Noise Control Eng J* 2010;58(2):145–56.
- [5] Franco F, De Rosa S, Polito T. Finite element investigations on the vibro-acoustic performance of plane plates with random stiffness. *Mech Adv Mater Struct* 2011;18(7):484–97.
- [6] Sorokin SV. Vibrations of and sound radiation from sandwich plates in heavy fluid loading conditions. *Compos Struct* 2000;48:219–30.
- [7] Zhang X, Li WL. A unified approach for predicting sound radiation from baffled rectangular plates with arbitrary boundary. *J Sound Vib* 2010;329(25):5307–20.
- [8] Bert CW, Kim CD, Birman V. Vibration of composite-material cylindrical shells with ring and/or stringer stiffeners. *Compos Struct* 1993;25:477–84.
- [9] Mittelstedt C, Beerhorst M. Closed-form buckling analysis of compressively loaded plates braced by omega-stringers. *Compos Struct* 2009;88:424–35.
- [10] Zhang ZF, Chen H, Ye L. Progressive failure analysis for advanced grid stiffened composite plates/shells. *Compos Struct* 2008;86:45–54.
- [11] Xin F, Lu TJ. Analytical modeling of wave propagation in orthogonally rib-stiffened sandwich structures: sound radiation. *Comput Struct* 2011;5–6(24):507–16.
- [12] Cao X, Hua H, Zhang Z. Sound radiation from shear deformable stiffened laminated plates. *J Sound Vib* 2011;330(16):4047–63.
- [13] Legault J, Mejdji A, Atalla N. Vibro-acoustic response of orthogonally stiffened panels: the effects of finite dimensions. *J Sound Vib* 2011;330(24):5928–48.
- [14] Xu H, Du J, Li WL. Vibrations of rectangular plates reinforced by any number of beams of arbitrary lengths and placement angles. *J Sound Vib* 2010;329(18):3759–79.
- [15] Cao X, Hua H, Zhang Z. Sound radiation from shear deformable stiffened laminated plates. *J Sound Vib* 2011;330:4047–63.
- [16] Xin FX, Lu TJ. Sound radiation of orthogonally rib-stiffened sandwich structures with cavity absorption. *Compos Sci Technol* 2010;70:2198–206.
- [17] Lomas NS, Hayek SI. Vibration and acoustic radiation of elastically supported rectangular plates. *J Sound Vib* 1977;52(1):1–25.
- [18] Berry A, Guyader JL, Nicolas J. A General formulation for the sound radiation from rectangular baffled plates with arbitrary boundary conditions. *J Acoust Soc Am* 1990;88(6):2792–802.
- [19] Yoo JW. Study on the general characteristics of the sound radiation of a rectangular plate with different boundary edge conditions. *J Mech Sci Technol* 2010;24(5):1111–8.
- [20] Zhang XF, Li WL. Vibrations of rectangular plates with arbitrary non-uniform elastic edge restraints. *J Sound Vib* 2009;326:221–34.
- [21] Li WL. Vibro-acoustic analysis of rectangular plates with elastic rotational edge restraints. *J Acoust Soc Am* 2006;120(2):769–79.
- [22] Li W. Sound radiation from rectangular plates with elastic boundary restraints. *J Acoust Soc Am* 2004;116(4):2520.
- [23] Jones RM. *Mechanics of composite material*. New York: McGraw-Hill Inc.; 1975.
- [24] LMS, version 4; 2010.
- [25] ANSYS 12.1, ANSYS, Inc., USA; 2010.